International Journal of Engineering Trends and Technology
ISSN: 2231–5381 / https://doi.org/10.14445/22315381/IJETT-V71I9P231

Volume 71 Issue 9, 356-366, September 2023

Original Article

A Multi-Period Approach to Background Leakage Estimation in Water Distribution Networks

Thabane H. Shabangu[1], Yskandar Hamam[1,2], Jaco A. Jordaan[1], Kazeem B. Adedeji[1]

[1]*Department of Electrical Engineering, Tshwane University of Technology, Pretoria, South Africa.*
[2]*ESIEE-Paris, Cité Descartes, Noisy-le-Grand, Paris, France*.

[1]*Corresponding Author : shabanguth@tut.ac.za*

Received: 14 April 2023 Revised: 05 June 2023 Accepted: 21 August 2023 Published: 03 September 2023

Abstract *- Localizing background leakage in a large-scale Water Distribution Network (WDN) presents a significant difficulty for water utilities. Leak localization has been the subject of several research projects; a comparison of the available methods reveals that the model-based method is less expensive and uses mathematical models to simulate the operation of the WDN. Due to this, they are better able to adjust to changes in the complexity of WDNs. The majority of model-based methods that have been suggested in the literature are only appropriate for burst-type leaks. However, for undetected background leakage, applying an appropriate hydraulic model permits the estimation of such leaks. Unfortunately, earlier studies in this direction did not consider the daily variations in water consumption, making it impossible to examine background leakage effectively. Specifically, under this, leak localization and analysis were considered for a single-period scenario. However, single-period monitoring of leak flow may occasionally result in incorrect results due to variations in water pressure between peak and off-peak hours. The multi-period analysis will, therefore, provide a more precise examination of the background leak estimate. In light of this, an improved leak localization method to address this shortcoming is proposed. The study will focus on the detection and localization of background leakage in WDNs, considering multi-period analysis. The multi-period analysis examines water consumption from 0 to 24 hours. This allows the analysis of water losses during both peak and off-peak water demand periods. The analysis is conducted on some water distribution networks adapted from real-life networks. The model is simulated, and leak flow and pressure head are observed within 24 hours of simulation. The variations in leak flow and pressure during this period are investigated.*

Keywords *- Leak flow, Multi-Period, Pressure-head, WDN, Water loss.*

1. Introduction

Pipelines are a sort of urban facility used to distribute water throughout cities. Efficient distribution across cities is challenged by the frequent water loss through leaks brought on by pipeline corrosion, cracks, and third-party interference [1]. Water distribution networks eventually experience frequent water loss, which seriously jeopardizes the systems' ability to function. This has been a serious problem facing utilities across the globe. The loss is closely related to, among other things, the expenses of fixing leaking pipes and environmental pollution [2, 3]. The latter has been a serious concern for public health. A water pipe network operating under low pressure may get infected by leaks [4–6]. The financial loss brought on by leakage is also enormous and varies greatly. For instance, McKenzie et al. [7] found that 37% of water loss in South Africa is attributable to leaks, with an estimated monetary value of more than R7 billion per year. The amount of water loss varies from one country to the next and from one WDN to the next regarding the waste of valuable natural resources. According to statistical research [8], the amount of water lost may approach 30% of the volume input. Water loss levels as high as 60% of the entire input volume may happen in extreme circumstances [9].

Additionally, according to a World Bank estimate of water losses, 48.6 billion m3/year of water is lost globally [10, 11]. Due to the effects of water losses, controlling water losses through pipe leakage detection and localization is a top priority for municipal water supply. Therefore, effective water loss control is essential. Given the magnitude and significance of WDNs as infrastructure, making wise decisions regarding leaks is crucial. To do this, an effective leak localization approach is necessary.

There are two major types of water losses in WDNs: reported and unreported losses [12]. The former includes pipe bursts and outflows from large openings, which are typically reported by utility staff or members of the public. The unreported loss is background loss, which is the outflow from

small cracks, joints, or pipe fittings. The burst type can be detected and localized [13, 14] by applying appropriate leakage detection methodology. This is because an evident pressure drop in the WDN characterizes them. Several research studies on detecting pipe bursts can be found in the literature. This ranges from the use of hardware-based methods [15-17] to model-based approaches [13, 18, 19]. However, background leakages are not detected by these approaches due to their diffuse nature.

Consequently, they contribute majorly to water loss volume within the pipe network when they occur for a very long time. Nevertheless, research studies have shown that losses due to background leaks can be modelled and estimated with the right hydraulic model. Unfortunately, studies on background leakage detection are very limited. In addition, the existing studies on background leakage detection do not consider consumer variations in water demand.

Because daily changes in water demand were not considered, we are optimistic that the existing studies in this field do not analyze background leakage very efficiently. Considering this, a research study to address this shortcoming is suggested.

WDNs are prone to background leakage, which results in water loss. Technically, practical WDNs cannot prevent a limited quantity of water loss. So, it is critical to minimize water losses to a manageable level. Indeed, studies on background leakage estimates are available, focusing on single-period analysis [20, 21].

However, consumer demand for water varies over time (with peak and off-peak periods), causing a change in the pressure at some nodes of the water networks. The pressure changes thus influence the estimate of background leakage due to leakage-to-pressure sensitivity. Hence, the background leakage during the peak water demand period will differ from that during the off-peak period.

Consequently, a single-period assessment may underestimate the background leakage flow along the system. Thus, to have a more realistic analysis of the background leakage estimate across the pipes, this paper analyses and discusses the leakage distribution over time. The background leakage is modelled using a graph-based integrated hydraulic model governed by the mass continuity and energy conservation laws and the pressure-to-leakage sensitivity.

The multi-period analysis reveals water consumption patterns from 0 to 24 hours, in contrast to conventional single-period modeling and estimation for background leakage flows in water distribution systems. This allows the analysis of water losses during both peak and off-peak water demand periods. The analysis was conducted on some water distribution networks adapted from real-life networks.

2. Materials and Methods

2.1. WDN Formulation under Leak-Free Scenario

Assume there are n_p pipes, n_j junction nodes (nodes with unknown heads), and n_f fixed-head nodes in a WDN. The nodes with unknown heads or pressure are referred to as junction nodes, also known as load nodes, whereas nodes with known heads or pressure are referred to as supply nodes, also known as fixed-head nodes. Thus, the total nodes in the network are expressed as

$$n_p = n_j + n_f \tag{1}$$

The flow through the network is guided by continuity equation, energy conservation and head loss (pressure drop) equations, respectively, described by Equation 2.

$$\left.\begin{aligned} EQ - A_s^T H - A_f^T H_f = 0 \\ A_s Q + d = 0 \end{aligned}\right\} \tag{2}$$

where $Q \in \Re^{np\times 1} = [Q_1, Q_2, ..., Q_{np}]^T$ is the vector of the pipe flow rate, $d \in \Re^{nj\times 1} = [d_1,d_2,.....,d_{nj}]^T$ is the vector of the base demand at the nodes with unknown heads/pressure, $H = [H_1,....., H_{nj}]^T$ represents the vector of the unknown heads/pressure across the load/junction nodes. It is of dimension ($n_j \times 1$), $H_f = [H_{f(1)}, ..., H_{f(nf)}]^T$ is the vector of the fixed head/pressure across the supply nodes. It is of dimension ($n_f \times 1$). In Equation 2, A_s represents the node-pipe connectivity matrix, which deals with the pipes connected to the junction/load nodes. It is of dimension ($n_j \times n_p$), and A_f represents the node-pipe connectivity matrix of dimension ($n_f \times n_p$), which deals with the pipes connecting to the fixed head/supply nodes.

Both A_s and A_f are obtained from the incidence matrix A as

$$A = \begin{bmatrix} A_s \\ A_f \end{bmatrix} \tag{3}$$

The element of A becomes -1 if the flow in pipe j is moving in the direction of node i, +1 if the flow is moving away from the node, and 0 otherwise. In Equation 2, E is a diagonal matrix whose elements are the partial derivatives of the flow within the pipe with respect to the pipe resistance, as described in Equation 4.

$$E = diag\left(r|Q|^{\alpha-1}\right) = \begin{bmatrix} r_1|Q_1|^{\alpha-1} & \cdots & \cdots & \cdots \\ \cdots & r_2|Q_2|^{\alpha-1} & \cdots & \cdots \\ \vdots & \vdots & \ddots & \vdots \\ \cdots & \cdots & \cdots & r_{n_p}|Q_{n_p}|^{\alpha-1} \end{bmatrix} \tag{4}$$

where $r = [r_1, ..., r_{np}]^T$ represents the pipe resistance vector, and α is an exponent whose value depends on the headloss model used. The r is computed using either the

Hazen-William or Darcy-Weisbach headloss model. The expressions in Equation 2 may also be written as

$$\begin{bmatrix} E & -A_s^T \\ A_s & 0 \end{bmatrix}\begin{bmatrix} Q \\ H \end{bmatrix}+\begin{bmatrix} -A_f^T H_f \\ d \end{bmatrix}=0 \tag{5}$$

It should be noted that the based demand d in Equation 5 is fixed and single period. Nodal demand varies with time depending on the type of consumer; thus, a more accurate analysis is to use a multi-period scenario where the base demand varies with time.

2.2. Modeling Water Demand Variation

The estimations produced from monthly water meter readings serve as the foundation for the node demand data used in a WDN study. Static distribution parameters that differ depending on the consumer type (residential, commercial, and industrial regions) make up the nodal demand profiles. To model demand variations with time, a set of demand multipliers is employed as the driving inputs [22]. Thus, at a given time t, the base demand is expressed as

$$d(t)=m(t)\times d \tag{6}$$

where $d(t) = [d_1(t),d_2(t),.....,d_{nj}(t)]^T$ is the vector of the time-varying demand at the node, $m(t) = (m_1(t),m_2(t),....., m_{nt}(t))$ is the set of demand multipliers at each time t and d represents the base demand at the node already defined. Thus, with the time-varying demand, Equation 5 may be rewritten as

$$\left.\begin{aligned} EQ(t)-A_s^T H(t)-A_f^T H_f(t)=0 \\ A_s Q(t)+d(t)=0 \end{aligned}\right\} \tag{7}$$

2.2. Inclusion of Pressure-Dependent Background Leakage Model

In WDNs, background leakage originates at nodes and along pipes where there are minor cracks or damaged joints. Studies [23–28] revealed that leak flow depends on pressure and must be modelled as pressure-dependent. Following a similar procedure by [21, 29], the pressure-dependent leakage relationship is often defined within the vector of the nodal leakage flow rate q_{nl} of dimension ($n_j \times 1$). Thus, by the inclusion of the leakage model, Equation 7 may be rewritten as

$$\left.\begin{aligned} EQ(t)-A_s^T H(t)-A_f^T H_f(t)=0 \\ A_s Q(t)+\{d(t)+q_{nl}(t)\}=0 \end{aligned}\right\} \tag{8}$$

A common assumption in leakage modeling within WDNs is that the end nodes of the pipe will account for half of the leakage flow. Thus, at time t, the nodal leakage vector ($q_{nl}(t)$) is related to the vector of leak flow along the pipe using

$$q_{nl}(t)=\frac{1}{2}\psi[Q_{leak}(t)]=\frac{1}{2}\psi\begin{bmatrix} Q_{1-leak}(t) \\ \vdots \\ Q_{np-leak}(t) \end{bmatrix} \tag{9}$$

where,

$$\psi=|A| \tag{10}$$

In Equation 9, $Q_{leak}(t) = [Q_{1-leak}(t), Q_{2-leak}(t), ...,Q_{np-leak}(t)]^T$ is the vector of the background leakage flow along the pipe at time t. Thus, background leakage flow along the pipe at each time step t is expressed as

$$Q_{leak}(t)=\begin{cases} \beta L\left(H_j(t)\right)^{\delta} & if \quad H_j(t)>0 \\ 0 & if \quad H_j(t)\le 0 \end{cases} \tag{11}$$

where β is the background leakage discharge coefficient along the pipe, L is the pipe length pipe, and δ represents the leak-to-pressure exponent. Previous studies [30] have shown that δ has a value of 1.18 for background leakage. $H_j(t)$ is the pressure head vector along the pipe at time t. This is computed as the mean of the pressure head values at its end nodes.

The $H_j(t)$ is computed as the mean of the pressure head values at the two ends of the pipe. This may be computed using the topological incidence matrix as

$$H_j(t)=\frac{1}{2}\psi^T H \tag{12}$$

Therefore, the expressions in Equation 8 may be conveniently written as

$$f(x)=f\begin{pmatrix} Q(t) \\ H(t) \end{pmatrix}=\begin{pmatrix} E & -A_s^T \\ A_s & 0 \end{pmatrix}\begin{pmatrix} Q(t) \\ H(t) \end{pmatrix}+\begin{pmatrix} -A_f^T H_f(t) \\ d(t)+q_{nl}(t) \end{pmatrix}=0 \tag{13}$$

Applying the Newton-Raphson (NR) iterative method to the expression $f(x) = f(Q(t), H(t)) = 0$, at every iteration "k", the estimate of the nodal pressure head and the flow rate through the pipe for each time step is derived from Equations 14 and 15 as

$$H^{(k+1)}(t)=\left(B(t)+N_{lk}(t)\right)^{-1}\begin{bmatrix} -\left\{A_s Q^{(k)}(t)+\left(d(t)+q_{nl}(t)\right)\right\}+ \\ N_{lk}(t)H^{(k)}(t)+A_s N^{-1}(t)\left\{E(t)Q^{(k)}(t)-A_f^T H_f(t)\right\} \end{bmatrix} \tag{14}$$

$$Q^{(k+1)}(t)=Q^{(k)}(t)-N^{-1}(t)\left(E(t)Q^{(k)}(t)-A_s^T H^{(k+1)}(t)\right) + N^{-1}(t)A_f^T H_f(t) \tag{15}$$

where B denotes the network admittance matrix defined as

$$B(t) = A_s N^{-1}(t) A_s^T \tag{16}$$

In Equations 14 and 15, $N(t)$ is a $(n_p \times n_p)$ diagonal matrix whose elements are the derivatives of the head loss component at time t, and $N_{lk}(t)$ is a diagonal matrix of size $(n_j \times n_j)$ whose elements are the derivatives of the nodal leakage vector $q_{nl}(t)$ at time t with respect to the pressure head along the pipe. Therefore, at each time step t, the elements of the matrix $N(t)$ for the pipes may be obtained as

$$N(t) = \begin{bmatrix} \alpha r_1 \left|Q_1(t)\right|^{\alpha-1} & \cdots & \cdots & \cdots \\ \cdots & \alpha r_2 \left|Q_2(t)\right|^{\alpha-1} & \cdots & \cdots \\ \vdots & \vdots & \ddots & \vdots \\ \cdots & \cdots & \cdots & \alpha r_{np} \left|Q_{np}(t)\right|^{\alpha-1} \end{bmatrix} \tag{17}$$

Also, at each time step t, the element of matrix $N_{lk}(t)$ gives.

$$N_{lk}(t) = \frac{1}{2}\psi\left[\frac{d}{dH_j} Q_{leak}(t)\right] = \frac{1}{2}\psi\begin{bmatrix} \frac{d}{dH_j} Q_{1-leak}(t) \\ \vdots \\ \frac{d}{dH_j} Q_{np-leak}(t) \end{bmatrix} \tag{18}$$

where,

$$\frac{d}{dH_j} Q_{leak}(t) = \begin{cases} \delta\beta L\left(H_j(t)\right)^{\delta-1} & if \quad H_j(t) > 0 \\ 0 & if \quad H_j(t) \le 0 \end{cases} \tag{19}$$

During the iterative process, the iteration is aborted when

$$\left|H^{(k+1)}(t) - H^{(k)}(t)\right| < tolerance \tag{20}$$

or when

$$\left|Q^{(k+1)}(t) - Q^{(k)}(t)\right| < tolerance \tag{21}$$

An error tolerance value of 10−5 was used as a stopping criterion in the iterative process. The multi-period analysis covers the period of 24 hours (from 0 to 24 hours). The model is simulated, and leak flow and the pressure head are observed within the 24-hour simulation time. The variations of the leak flow and pressure are analyzed and discussed.

3. Simulation Results and Discussion

3.1. Case Study Network I

This network (see Figure 1) was adapted from [31]. As shown in Figure 1, it has 12 pipes of the same length, 1 *km* each. 9 nodes connect the pipes. An elevated reservoir serving as the fixed-head node and having a total head of 100 *m* provides water by gravity. The pipes range in diameter from 100 *mm* to 250 *mm*. Base demand ranges between 62.5 *l/s* and 208.1 *l/s* at the various junction nodes. The Hazen-Williams model is employed to estimate head loss. For all pipes combined, the Hazen-Williams coefficient is 130. The hydraulic information pertinent to this network is illustrated in Tables 1 and 2 [31].

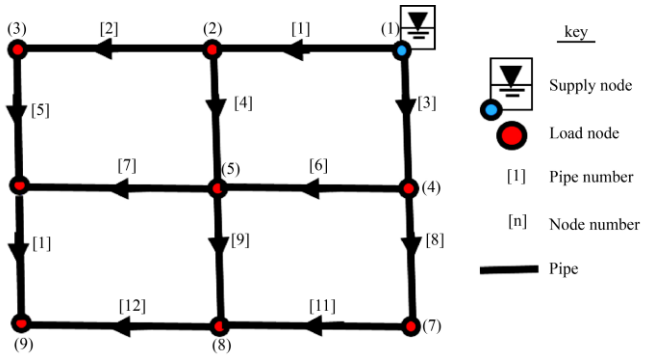

Fig. 1 The layout of the case study network I

Table 1. Pipe parameters for the case study network I

Pipe ID	Start Node	End Node	Length (*m*)	Diameter (*mm*)
1	1	2	1000	250
2	2	3	1000	175
3	1	4	1000	250
4	2	5	1000	145
5	3	6	1000	115
6	4	5	1000	145
7	5	6	1000	100
8	4	7	1000	175
9	5	8	1000	100
10	6	9	1000	100
11	7	8	1000	115
12	8	9	1000	100

Table 2. Node parameters for the case study network I

Node ID	Elevation (*m*)	Demand (*l/s*)
1	100	208.1
2	30	20.8
3	30	20.8
4	30	20.8
5	30	20.8
6	30	20.8
7	30	20.8
8	30	20.8
9	30	62.5

Figure 2 shows the variability of the pressure head at the nodes during the 24-hour observation period. This analysis was conducted for nodes 1 to 4 (Figure 2(a)) and nodes 5 to 9 (Figure 2(b)). As can be observed in Figure 2(a), the pressure head at node 3 changes greatly between 25 *m* and 88 *m*, with a wide difference of 63 *m* within 24 hours. The variations of the pressure through nodes 2 and 4 are small compared to those of node 3, while node 1 is observed to be the same throughout the period. This is expected as node 1 represents the supply node with a fixed head. Aside from the supply node, nodes 5 and 7 (Figure 2(b)) experienced the least pressure variation during the 24-hour period. In Figure 2(a), node 3 experiences the lowest pressure throughout the 24-hour observation period, with the least occurring at 19 hours, while the maximum pressure occurs between 1 and 3 a.m. This same trend is observed for nodes 2 and 4. In Figure 2(b), the pressure head profile through node 9 exhibits a similar trend to that of node 3. However, in most of the periods, node 9 becomes pressure deficient. Aside from 1, 3, 4, and 5 hours, the rest of the period indicates a pressure-deficient condition for node 9, as seen with the negative pressure values. During this condition, the pressure becomes insufficient to supply the necessary demand at this node. The flow at this node during these periods is expected to be extremely low. As can be seen in Figure 3, this node experiences the lowest leak flow during these periods. Nodes 5 and 7 (Figure 2(b)) also had no pressure-deficient conditions for the entire 24-hour observation period. For all the nodes, the pressure is observed to be nearly constant between 3 a.m. and 5 a.m. Figure 3 shows the leak flow through the node during the 24-hour observation period for case study network I. The flow variation with time through node 1 is almost linear, while the flow rate through nodes 3, 2, and 4 varies greatly with time. Similar to the results presented in Figure 2, the time changes greatly affect the leak flow through node 3. Nodes 2 and 4 have the highest leak flow, with the least leak discharge occurring at 7 a.m. and 7 p.m. The same is observed for nodes 3 and 1. In Figure 3(b), node 9 has the least leak flow. Within 24 hours, the leak flow through node 9 is zero during most of the observation period (about 18 hours), while it has maximum leak flow between 3 a.m. and 5 a.m. Node 5 has the highest leak flow, which occurs most of the time.

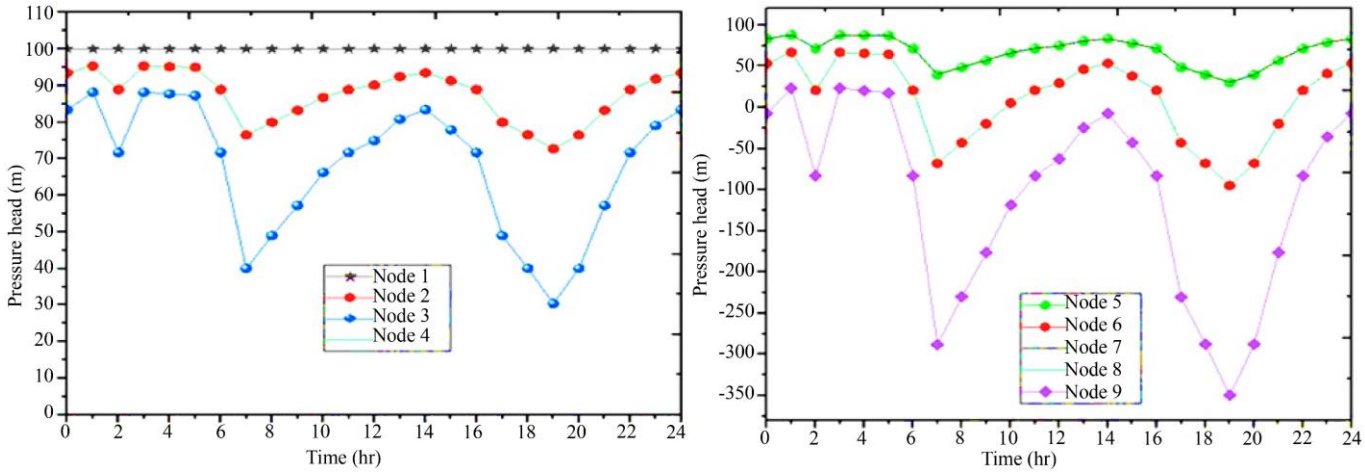

Fig. 2 Profile of the nodal pressure-head for network I through (a) Nodes 1 to 4 and (b) Nodes 5 to 9

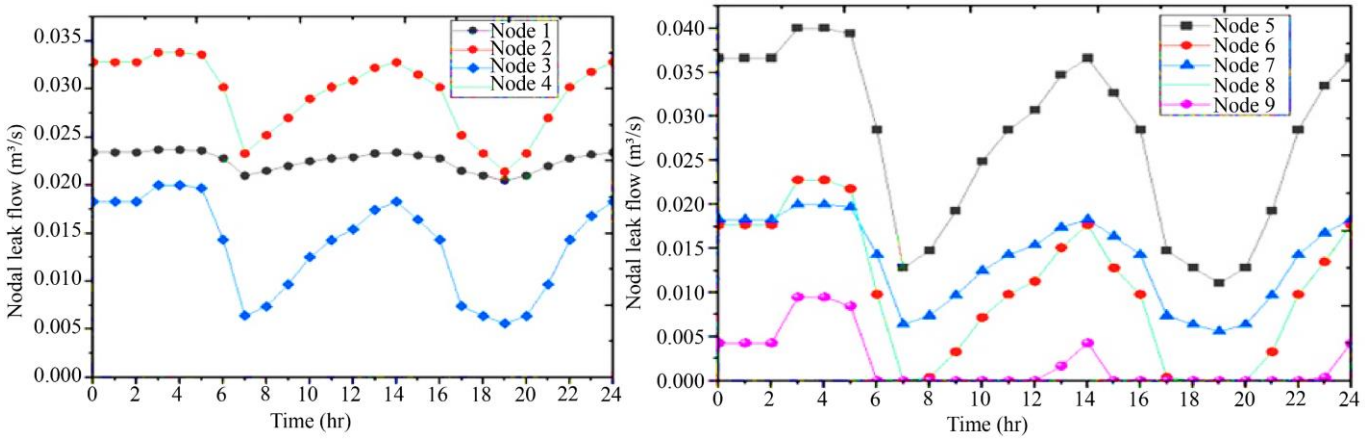

Fig. 3 Nodal leak flow for network I through (a) Nodes 1 to 4 and (b) Nodes 5 to 9

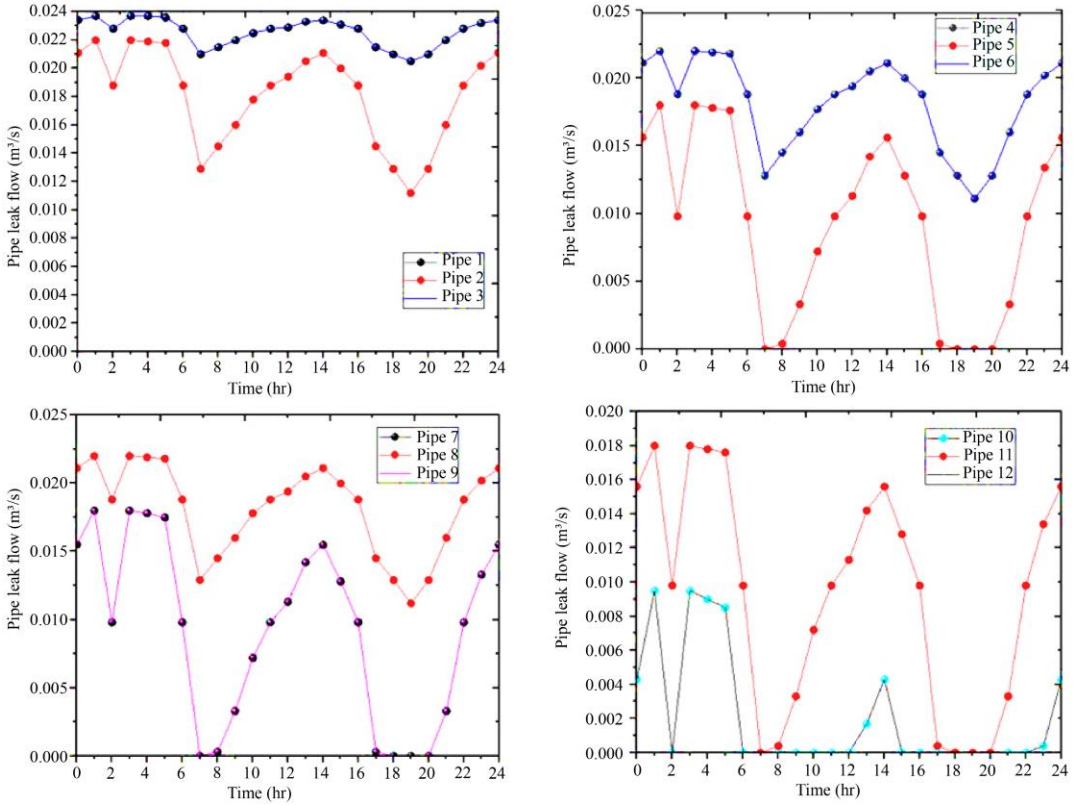

Fig. 4 Pipe leak flow for network I through (a) Pipes 1 to 3, (b) Pipes 4 to 6, (c) Pipes 7 to 9, and (d) Pipes 10 to 12

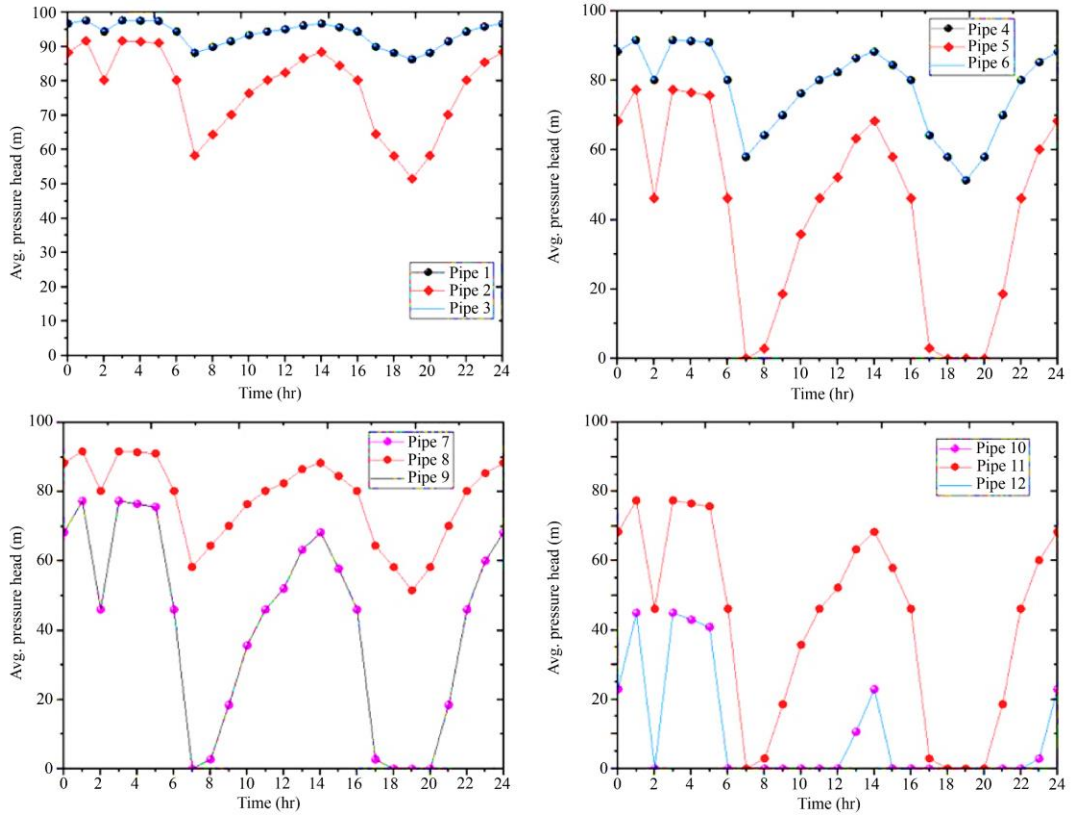

Fig. 5 The average pressure-head through the pipes for network I through (a) Pipes 1 to 3, (b) Pipes 4 to 6, (c) Pipes 7 to 9, and (d) Pipes 10 to 12

Nevertheless, the occurrence of its minimum leak flow was observed at 7 a.m., 6 p.m., 7 p.m., and 8 p.m., respectively. Among these nodes, node 5 is the most sensitive node, as the leak flow variation with time through this node is the most significant. It also had the highest leak flow during most of the 24-hour observation.

Figure 4 presents the leak flow through the pipe during the 24-hour observation period for the case study network I. It is observed that the leak flow through pipes 5, 7, 9, 10, 11 and 12 is greatly affected by the time variation. Even though pipes 1 and 3 have the highest leak flow rate, the leak flow rate variations due to these pipes are the least sensitive to time changes. Furthermore, some of the pipes had no leakage for a brief period. For example, pipes 10 and 12 (Figure 4(d)) experience zero leakage during the majority of the 24-hour observation period, while pipes 5 (Figure 4(b)) have zero leakage for a short period. Figure 5 shows the profile of the average pressure head through the pipe during the 24-hour period for the case study network I.

Similar to the findings in Figure 4, average pressures in pipes 1 and 3 (Figure 5(a)) are the least sensitive to time variation, whereas average pressures in pipes 5, 7, 9, 10, 11, and 12 are greatly affected by time variation. Also, pipes 1 and 3 have the highest pressure. This pressure is sufficient to produce a higher leak flow rate in these pipes, as observed in Figure 4(a). Only pipes 10 and 12 (Figure 5(d)) had the lowest pressure during the 24-hour period. Some of these pipes, such as pipe 5 (Figure 5(b)), pipes 7 and 9 (Figure 5(c)), and pipes 10, 11, and 12 (Figure 5(d)), had zero pressure within some periods of observation. This accounts for the reason why the leak flow through them is zero during these periods.

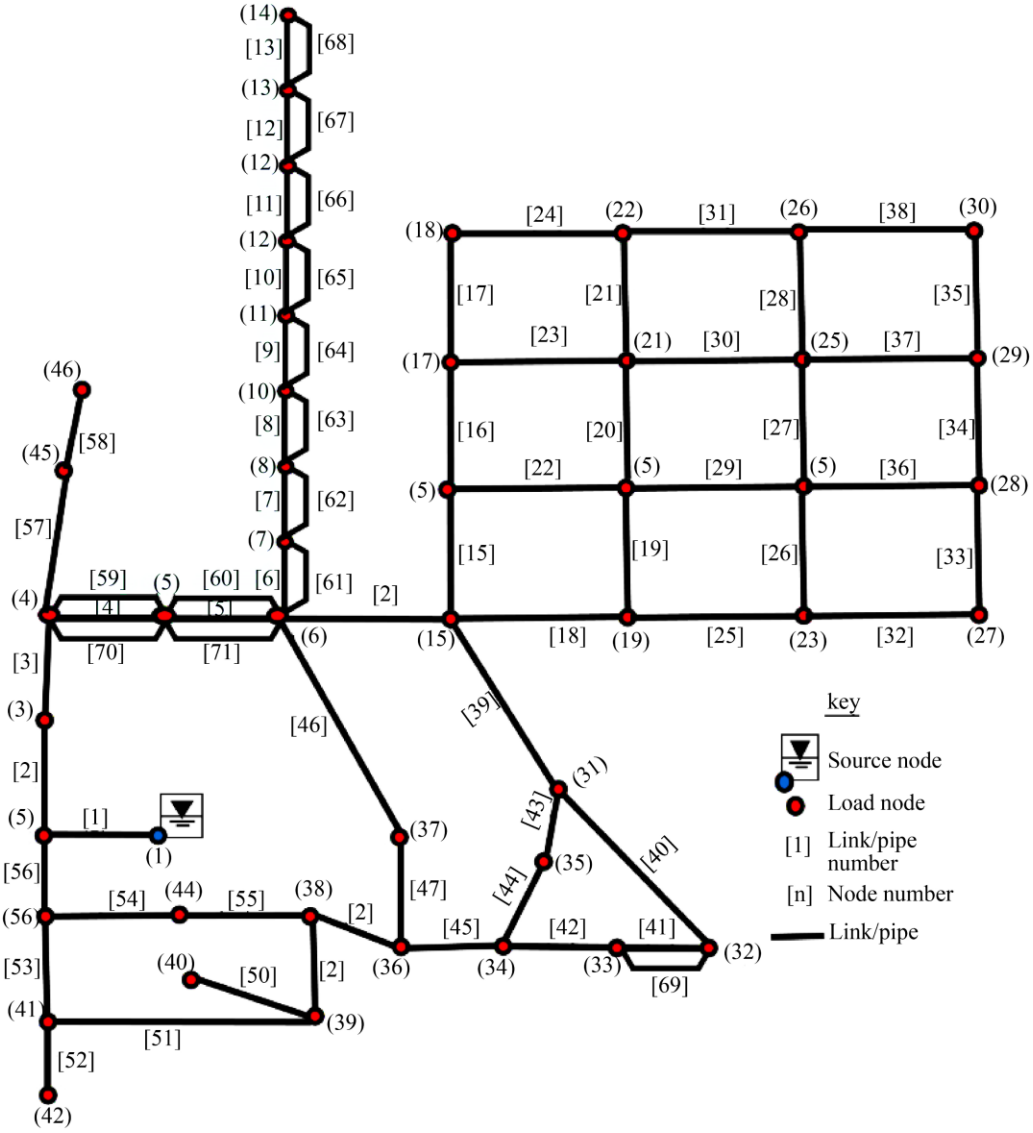

Fig. 6 Case study water network II used for the numerical examples

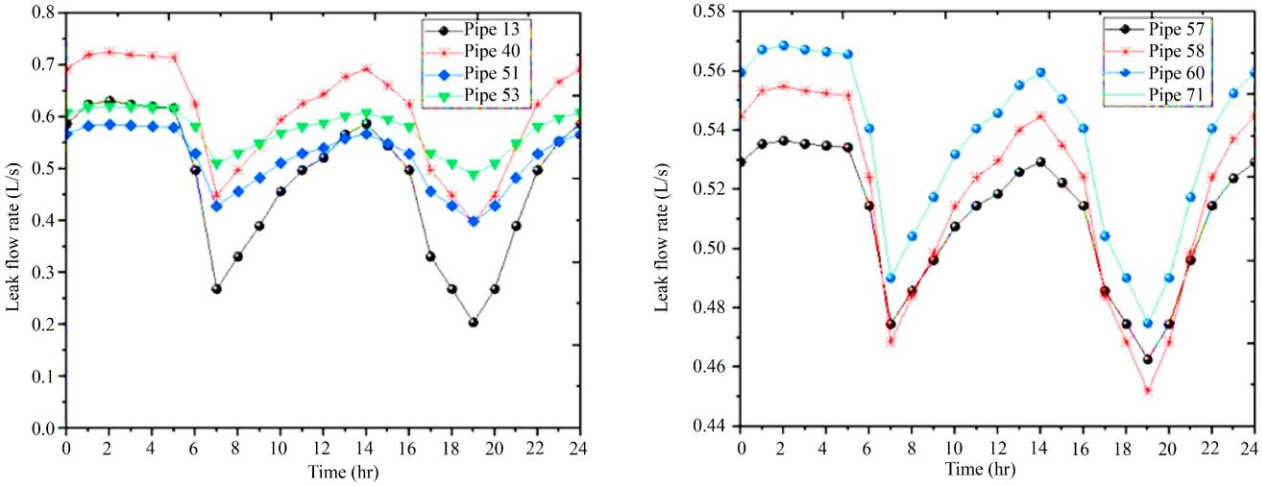

Fig. 7 Profile of the pipe leak flow for network II

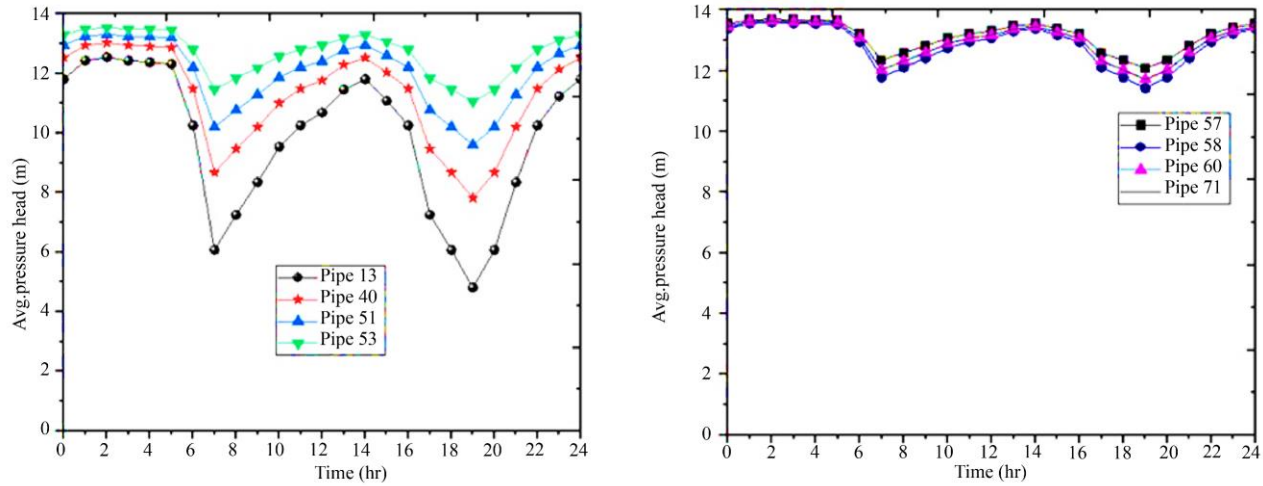

Fig. 8 Average pressure head through the pipes for network II

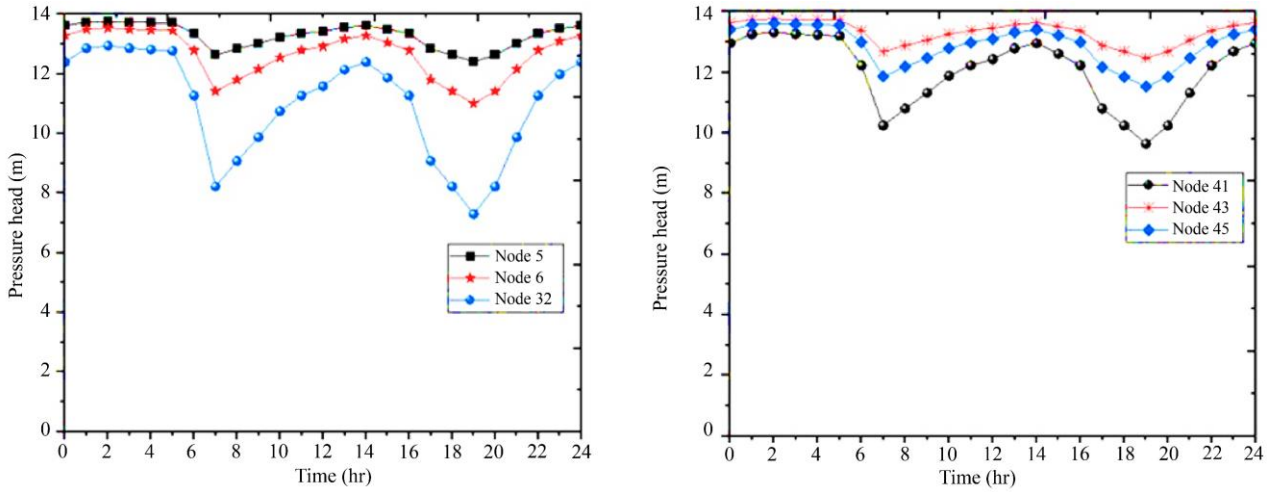

Fig. 9 Profile of the nodal pressure head for network II for (a) nodes 5, 6 and 32 (b) nodes 41, 43 and 45

3.2. Case Study Network II

Figure 6 shows the topology of the water network II used for the investigation. The authors in [32] previously used this network for state estimation in the WDNs. It is a real WDN in a particular zone in a small municipality in southern India. As may be observed in Figure 6, the network has 46 nodes, out of which 1 is a fixed-head node (represented by a reservoir) and 45 junction nodes. The fixed-head node (node 1) and the junction nodes (which index from node 2 to node 46) are interconnected by a series of pipes of varying lengths and diameters between 25 *m* and 300 *m* and 80 *mm* and 300 *mm*, respectively. The base demand at the junction nodes varies between 0.19 *l/s* and 12.4 *l/s*. Hazen-William's model is used for the head loss estimation. The Hazen-William's coefficient for all the pipes is equal to 120. The water level in the reservoir at node 1 (the fixed-head node) equals 14 *m*. The elevation at all other nodes (that is, the junction nodes) is taken as zero. The hydraulic data relevant to this network can be found in [21, 32]. For this network, the leak flow and pressure through the critical pipes and nodes reported in [21] are analyzed over the 24-hour observation period. Figure 7 shows the leak flow through the pipe during the 24-hour observation period for case study network II. It is observed that the leak flow through pipes 13 and 40 (Figure 7(a)) and 57, 58, 60, and 71 (Figure 7(b)) is very sensitive to time variation, changing significantly over 24 hours, whereas the leak flow through pipe 53 is the least sensitive to this variation. Also, the leak flow is almost constant during some parts of the observation time. This is observed between 1 a.m. and 5 a.m. for all the pipes. Figure 7(a) shows that the leak flow through pipe 13 is relatively higher than that of pipes 51 and 53 for some periods (between 1 a.m. and 5 a.m.), while it is relatively lower for the rest of the period. The leak flow through the pipes analyzed in Figure 7(b) exhibits a somewhat similar trend. Figure 8 presents the profile of the average pressure head through the pipe during the 24-hour observation period for the case study network II. Similarly to the results shown in Figure 7, the pressure in pipes 13 and 40 (Figure 8(a)) is very sensitive to time variation, changing significantly over a 24-hour period, whereas the pressure through the pipes in Figure 8(b) is less sensitive to this variation.

Also, the pressure is almost constant during some parts of the observation time between 1 a.m. and 5 a.m. for all the pipes. Pipes 57, 58, 60, and 71 (Figure 8(b)) are also observed to have higher pressure than some of the pipes in Figure 8(a). Also, the pressure through the pipes exhibits a similar trend throughout the observation period. Figure 9 shows the variability of the pressure head at the nodes during 24 hours for the case study network II. This analysis was conducted for nodes 5, 6, and 32 (Figure 9(a)) and nodes 41, 43, and 45 (Figure 9(b)). As shown in Figure 9(a), node 32 is very sensitive to time changes because the pressure head varies greatly between 7 *m* and 13 *m* during the 24-hour observation period, whereas node 5 is the least sensitive. After all, only a slight variation in pressure values was observed during the observation period. In Figure 9 (b), nodes 43 and 45 have the least pressure variation, while node 41 follows the same pattern as node 32 in Figure 9 (a). Also, all the nodes exhibited higher pressures during most of the observation period. As shown in Figure 9, the lowest pressures occur only at 7 a.m. and 7 p.m. Also, the highest pressure occurred in nodes 5 and 43, while node 32 had the least pressure. This trend is observed throughout the 24-hour observation period.

4. Conclusion

Water loss from leaking pipes in water piping systems is a major issue for water utilities globally. The problem becomes more frustrating when a leak occurs at multiple locations along a single pipe in the system. Nevertheless, studies on leak detection due to background loss are available, focusing on single-period situations where the base demand is assumed to be fixed. A single-period analysis may underestimate the leak estimate in water distribution networks since water demand at the node varies with time due to consumer demand. This paper presents a multi-period approach to leak estimation due to background loss. The multi-period analysis covers water consumption patterns from 0 to 24 hours, in contrast to conventional single-period modeling and estimation for background leakage flows in water distribution systems. This allows the analysis of water losses during both peak and off-peak water demand periods. The analysis was conducted on some WDNs adapted from real-life networks. The model is simulated, and leak flow and pressure head are observed within 24 hours of simulation. The variations in leakage as well as pressure are investigated. The results show that during the observation periods, some of the flow and pressure in some of the pipes and nodes were very sensitive to time changes, with a wide variation. The analysis also shows that some nodes exhibit pressure-deficient conditions during a few periods, while the pressure is relatively higher during other periods. The results indicate that multi-period analysis provides a more accurate and extensive analysis of the leak flow profile through the pipes in the network.

Acknowledgments

The authors acknowledged the support from the Tshwane University of Technology, Pretoria, South Africa.

References

[1] L. Berardi et al., "Development of Pipe Deterioration Models for Water Distribution Systems using EPR," *Journal of Hydroinformatics*, vol. 10, no. 2, pp. 113-126, 2008. [CrossRef] [Google Scholar] [Publisher Link]

[2] R. Puust et al., "A Review of Methods for Leakage Management in Pipe Networks," *Urban Water Journal*, vol. 7, no. 1, pp. 25-45, 2010. [CrossRef] [Google Scholar] [Publisher Link]

[3] Joaquim Sousa et al., "Locating Leaks in Water Distribution Networks with Simulated Annealing and Graph Theory," *Procedia Engineering*, vol. 119, pp. 63-71, 2015. [CrossRef] [Google Scholar] [Publisher Link]

[4] Xuli Meng et al., "Improved Stormwater Management through the Combination of the Conventional Water Sensitive Urban Design and Stormwater Pipeline Network," *Process Safety and Environmental Protection*, vol. 159, pp. 1164-1173, 2022. [CrossRef] [Google Scholar] [Publisher Link]

[5] Lu Chang, Joseph H.W. Lee, and Y.S. Fung, "Prediction of Lead Leaching from Galvanic Corrosion of Lead-Containing Components in Copper Pipe Drinking Water Supply Systems," *Journal of Hazardous Materials*, vol. 436, 2022. [CrossRef] [Google Scholar] [Publisher Link]

[6] Peter Jarvis, and John Fawell, "Lead in Drinking Water–An Ongoing Public Health Concern?," *Current Opinion in Environmental Science & Health*, vol. 20, 2021. [CrossRef] [Google Scholar] [Publisher Link]

[7] R.S. McKenzie, Z. Siqalaba, and W. Wegelin, *The State of Non-Revenue Water in South Africa*, South Africa: Water Research Commission, 2012. [Google Scholar] [Publisher Link]

[8] EPA, *Control and Mitigation of Drinking Water Losses in Distribution Systems*, United States Environmental Protection Agency, USA, 2010. [Google Scholar] [Publisher Link]

[9] Malcolm Farley, *Leakage Management and Control- A Best Practice Manual*, Geneva, Switzerland: World Health Organization, 2001. [Google Scholar] [Publisher Link]

[10] Julian Thornton, Reinhard Sturm, and George Kunkel, *Water Loss Control*, 2nd edition, New York: McGraw Hill Professional, 2008. [Google Scholar] [Publisher Link]

[11] Chan-Wook Lee, and Do-Guen Yoo, "Development of Leakage Detection Model and Its Application for Water Distribution Networks using RNN-LSTM," *Sustainability*, vol. 13, no. 16, pp. 1-15, 2021. [CrossRef] [Google Scholar] [Publisher Link]

[12] Carmine Covelli et al., "Reduction in Water Losses in Water Distribution Systems using Pressure Reduction Valves," *Water Science and Technology-Water Supply*, vol. 16, no. 4, pp. 1033-1045, 2016. [CrossRef] [Google Scholar] [Publisher Link]

[13] Hyeong-Suk Kim et al., "Development of the Methodology for Pipe Burst Detection in Multi-Regional Water Supply Networks using Sensor Network Maps and Deep Neural Networks," *Sustainability*, vol. 14, no. 22, 2022. [CrossRef] [Google Scholar] [Publisher Link]

[14] Jeongwook Choi, Gimoon Jeong, and Doosun Kang, "Multiple Leak Detection in Water Distribution Networks Following Seismic Damage," *Sustainability*, vol. 13, no. 15, 2021. [CrossRef] [Google Scholar] [Publisher Link]

[15] Majid Ahadi, and Mehrdad Sharif Bakhtiar, "Leak Detection in Water-Filled Plastic Pipes through the Application of Tuned Wavelet Transforms to Acoustic Emission Signals," *Applied Acoustics*, vol. 71, no. 7, pp. 634-639, 2010. [CrossRef] [Google Scholar] [Publisher Link]

[16] A. De Coster et al., "Towards an Improvement of GPR-Based Detection of Pipes and Leaks in Water Distribution Networks," *Journal of Applied Geophysics*, vol. 162, pp.138-151, 2019. [CrossRef] [Google Scholar] [Publisher Link]

[17] Samer El-Zahab, Eslam Mohammed Abdelkader, and Tarek Zayed, "An Accelerometer-Based Leak Detection System," *Mechanical Systems and Signal Processing*, vol. 108, pp. 276-291, 2018. [CrossRef] [Google Scholar] [Publisher Link]

[18] Myrna V. Casillas Ponce, Luis E. Garza Castañón, and Vicenç Puig Cayuela, "Model-Based Leak Detection and Location in Water Distribution Networks Considering an Extended-Horizon Analysis of Pressure Sensitivities," *Journal of Hydroinformatics*, vol. 16, no. 3, pp. 649-670, 2014. [CrossRef] [Google Scholar] [Publisher Link]

[19] Ahmad Momeni, and Kalyan R. Piratla, "A Proof-of-Concept Study for Hydraulic Model-Based Leakage Detection in Water Pipelines using Pressure Monitoring Data," *Frontiers in Water*, vol. 3, pp. 1-15, 2021. [CrossRef] [Google Scholar] [Publisher Link]

[20] Shrikrishna Hingmire et al., "Probing to Reduce Operational Losses in NRW by using IoT," *SSRG International Journal of Electrical and Electronics Engineering*, vol. 10, no. 6, pp. 23-32, 2023. [CrossRef] [Google Scholar] [Publisher Link]

[21] K. B. Adedeji, "*Development of a Leakage Detection and Localisation Technique for Real-Time Applications in Water Distribution Networks*," PhD Thesis, Department of Electrical Engineering, Tshwane University of Technology, Pretoria, South Africa, 2018. [Google Scholar]

[22] M. Nivetha, and S. Sundaresan, "Automated Drinking Water Distribution using Arduino," *SSRG International Journal of Civil Engineering*, vol. 4, no. 5, pp. 66-69, 2017. [CrossRef] [Google Scholar] [Publisher Link]

[23] Özgür Özdemir et al., "Analysis of the Effect of Pressure Control on Leakages in Distribution Systems by¨ FAVAD Equation and Field Applications," *Water Practice and Technology*, vol. 16, no. 2, pp. 320–332, 2016. [CrossRef] [Google Scholar] [Publisher Link]

[24] Irene Marzola, Stefano Alvisi, and Marco Franchini, "Analysis of MNF and FAVAD Models for Leakage Characterization by Exploiting Smart-Metered Data: The Case of the Gorino Ferrarese (FE-Italy) District," *Water*, vol. 13, no. 5, pp. 1-15, 2021. [CrossRef] [Google Scholar] [Publisher Link]

[25] Débora Alves et al., "Robust Data-Driven Leak Localization in Water Distribution Networks using Pressure Measurements and Topological Information," *Sensors*, vol. 21, no. 22, pp. 1-19, 2021. [CrossRef] [Google Scholar] [Publisher Link]

[26] Juan Li et al., "A Novel Multi-Leak Sensor Deployment Strategy in Water Distribution Networks based on the LSDR-JMI Method," *Control Engineering Practice*, vol. 107, 2021. [CrossRef] [Google Scholar] [Publisher Link]

[27] Sajid Ali, Muhammad A. Hawwa, and Uthman Baroudi, "Effect of Leak Geometry on Water Characteristics Inside Pipes," *Sustainability*, vol. 14, no. 9, pp. 1-21, 2022. [CrossRef] [Google Scholar] [Publisher Link]

[28] Anirudh Nagaraj et al., "Leak Detection in Smart Water Grids using EPANET and Machine Learning Techniques," *IETE Journal of Education*, vol. 62, no. 2, pp. 71–79, 2021. [CrossRef] [Google Scholar] [Publisher Link]

[29] Orazio Giustolisi, Dragan Savic, and Zoran Kapelan, "Pressure-Driven Demand and Leakage Simulation for Water Distribution Networks," *Journal of Hydraulic Engineering*, vol. 134, no. 5, pp. 1–39, 2008. [CrossRef] [Google Scholar] [Publisher Link]

[30] George Germanopoulos, "A Technical Note on the Inclusion of Pressure Dependent Demand and Leakage Terms in Water Supply Network Models," *Civil Engineering Systems*, vol. 2, no. 3, pp. 171–179, 1985. [CrossRef] [Google Scholar] [Publisher Link]

[31] Massoud Tabesh et al. "A Comparative Study between the Modified and Available Demand Driven Based Models for Head-Driven Analysis of Water Distribution Networks," *Urban Water Journal*, vol. 11, no. 3, pp. 221–230, 2014. [CrossRef] [Google Scholar] [Publisher Link]

[32] S. Mohan Kumar, Shankar Narasimhan, and S. Murty Bhallamudi, "State Estimation in Water Distribution Networks using Graph-Theoretic Reduction Strategy," *Journal of Water Resources Planning and Management*, vol. 134, no. 5, pp. 395-403, 2008. [CrossRef] [Google Scholar] [Publisher Link]